Electron Paramagnetic Resonance Measurements of the Ferrous Mononuclear Site of Phthalate Dioxygenase Substituted with Alternate Divalent Metal Ions: Direct Evidence for Ligation of Two Histidines in the Copper(II)-Reconstituted Protein†

Eric D. Coulter,‡,§ Namdoo Moon,‖ Christopher J. Batie,‡,⊥ William R. Dunham,‖ and David P. Ballou*,‡

Department of Biological Chemistry, University of Michigan, Ann Arbor, Michigan 48109-0606, and Biophysics Research Division, University of Michigan, Ann Arbor, Michigan 48109-1055

Received February 25, 1999; Revised Manuscript Received June 7, 1999

ABSTRACT: The metalloenzyme phthalate dioxygenase (PDO) contains two iron-based sites. A Rieske-type [2Fe-2S] cluster serves as an electron-transferring cofactor, and a mononuclear iron site is the putative site of substrate oxygenation. A reductase, which contains FMN and a plant-type [2Fe-2S] ferredoxin domain, transfers electrons from NADH to the Rieske center. Any of the metal ions, Fe(II), Cu(II), Co(II), Mn(II), and Zn(II), can be used to populate the mononuclear site, but only Fe(II) is competent for effecting hydroxylation. Nevertheless, studies of how these metal ions affect both the EPR spectra of the reduced Rieske site and the kinetics of electron transfer in the PDO system indicated that each of these metal ions binds tightly and affects the protein similarly. In this study, EPR spectra were obtained from samples in which iron of the mononuclear site was replaced with Cu(II). The use of ^{63}Cu(II), in combination with PDO obtained from cultures grown on media enriched in ^{15}N [using $(^{15}NH_4)_2SO_4$ as a sole nitrogen source], [δ,ϵ-^{15}N]histidine, as well as natural abundance sources of nitrogen, enabled detailed spectral analysis of the superhyperfine structure of the Cu(II) EPR lines. These studies clearly show that two histidines are coordinated to the mononuclear site. Coupled with previous studies [Bertini, I., Luchinat, C., Mincione, G., Parigi, G., Gassner G. T., and Ballou, D. P. (1996) *J. Bioinorg. Chem. 1,* 468−475] that show the presence of one or two water molecules coordinated to the iron, it is suggested that the mononuclear site is similar to several other mononuclear nonheme iron proteins, including naphthalene dioxygenase, for which crystal structures are available. The lack of observable EPR interaction signals between Cu(II) in the mononuclear site and the reduced Rieske center of PDO suggest that the two sites are at least 12 Å apart, which is similar to that found in the naphthalene dioxygenase crystal structure.

Aromatic compounds that are deposited in the soil by natural processes, such as the degradation of lignin, or by unnatural processes, such as industrial waste, can often be utilized as sources of energy and carbon by a variety of soil microorganisms (*1, 2*). The pathways by which bacterial systems metabolize inert aromatic compounds are thereby valuable as potential tools for bioremediation efforts. In soil, aerobic cleavage of the benzene ring is often initiated by the incorporation of both atoms of molecular oxygen directly into the benzene ring (*3*). As shown below, this requires 1 mol each of oxygen and NADH. These difficult oxygenations are frequently catalyzed by mononuclear nonheme iron dioxygenases (for reviews, see refs *3* and *4*). The resulting nonaromatic dihydrodiols are oxidized by dehydrogenases to form more highly activated catechols, with regeneration of NADH. The catechols are then cleaved by catechol dioxygenases (*4*). Benzene (*5*), benzoate (*6*), toluene (*7*), naphthalene (*8*), and phthalate (*9, 10*) are representative of a variety of compounds (more than 20 such similar systems are known) that can be metabolized in this way.

Phthalate-degrading systems have been identified in several organisms and are found to employ a common metabolic pathway (*11*−*13*). The phthalate dioxygenase system (PDOS)[1] studied in this work catalyzes the first step in the degradation of phthalate by *Bulkholderia cepacia*.[2] PDOS catalyzes the dihydroxylation of phthalate, forming

† Supported in part by the NIH (Grants GM-20877 to D.P.B. and GM-32785 to W.R.D.).

* To whom correspondence should be addressed: phone (734) 764-9582; fax (734) 763-4581; e-mail dballou@umich.edu.

‡ Department of Biological Chemistry, University of Michigan.

§ Present address: Department of Chemistry, University of Georgia, Athens, GA.

‖ Biophysics Research Division, University of Michigan.

⊥ Present address: Novartis, Research Triangle Park, NC.

[1] Abbreviations: PDO, phthalate dioxygenase from *Bulkholderia cepacia*; apoPDO, phthalate dioxygenase with the mononuclear metal ion removed; Fe(II)PDO, Cu(II)PDO, Co(II)PDO, Mn(II)PDO, and Zn(II)PDO, phthalate dioxygenase reconstituted at the mononuclear site with Fe(II), Cu(II), Co(II), Mn(II), and Zn(II), respectively; Fe(III)-PDO, ferric adduct of phthalate dioxygenase; PDOS, phthalate dioxygenase system consisting of PDO and phthalate dioxygenase reductase; PDR, phthalate dioxygenase reductase; [^{14}N]PDO, phthalate dioxygenase in which all nitrogen atoms are ^{14}N; [^{15}N]PDO, phthalate dioxygenase in which all nitrogen atoms are ^{15}N; [$^{15}N_2$]His-PDO, phthalate dioxygenase in which only the nitrogen atoms of histidine are ^{15}N and all others are ^{14}N; EXAFS, extended X-ray absorption fine structure spectroscopy; MCD, magnetic circular dichroism spectroscopy; ESEEM, electron spin−echo modulation spectroscopy; EPR, electron paramagnetic resonance spectroscopy; NMRD, nuclear magnetic resonance dispersion.

10.1021/bi9904499 CCC: $18.00
Published on Web 07/29/1999

Scheme 1

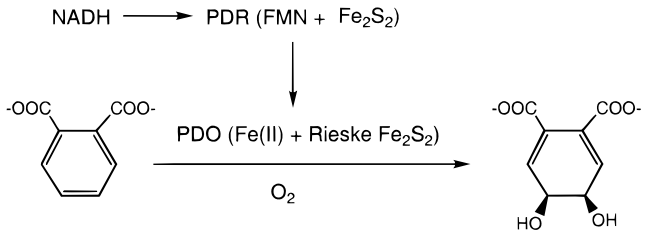

exclusively *cis*-4,5-dihydroxydihydrophthalate (1,2-dihydroxy-4,5-dicarboxy-3,5-cyclohexadiene), as shown in Scheme 1. PDOS is a two-component enzyme system composed of a 36 kDa monomeric phthalate dioxygenase reductase (PDR) and a 200 kDa tetrameric (α_4) terminal dioxygenase (PDO) (*14*). PDR shuttles electrons from NADH via an associated flavin (FMN) cofactor and a ferredoxin-type [2Fe-2S] cluster (*15*, *16*) to PDO. On the basis of number and identity of its cofactors, the PDOS belongs to the Class IA multicomponent Rieske center nonheme iron oxygenases as defined by Batie et al. (*17*).

Each subunit of PDO has been shown to contain three irons; two are involved in a [2Fe-2S] cluster, and the third, Fe(II), binds at a distinct site that is proposed to be the site of substrate oxygenation (*14, 18*). The visible and EPR spectra of all such oxygenases examined are very similar and are dominated by the Rieske [2Fe-2S] center (*19*). The physical properties of the [2Fe-2S] cluster of PDO (and of all of the mononuclear nonheme iron dioxygenases mentioned above) are quite different from those of typical plant-type ferredoxins, such as that present in PDR. Instead, this type of [2Fe-2S] center closely resembles the Rieske centers of respiratory chains; consequently, these mononuclear nonheme iron dioxygenases are often referred to as Rieske oxygenases. Rieske centers in both dioxygenases and respiratory chains exhibit high midpoint redox potentials (−100 to +400 mV) and low average EPR *g*-values ($g_{av} \sim 1.91$) compared to the [2Fe-2S] clusters of plant ferredoxins (−450 to −150 mV and $g_{av} \sim 1.96$) [for a review of the physical properties of [2Fe-2S] clusters, see Fee et al. (*20*)]. The distinguishing properties of Rieske [2Fe-2S] centers are now known to reflect the replacement of two cysteinate residues by two less electron-donating histidines as ligands to one of the iron atoms of the cluster. The structure of the PDO Rieske center has been extensively characterized by ENDOR (*21*−*23*), electron spin−echo modulation (ESEEM) (*24*), resonance Raman (*25*), and EXAFS (*26*) spectroscopies. These studies have confirmed the ligation of one iron by two histidines and the other by two cysteines (*21*−*24*) and have shown that the [2Fe-2S] core has the same dimensions as the plant-type [2Fe-2S] centers (*26*).

The recently determined three-dimensional structure of the related dioxygenase, naphthalene dioxygnenase (NDO) (*27*), has provided invaluable insight into the structures of both Rieske and mononuclear nonheme iron sites. The crystallographically determined Rieske site is in close agreement with the structure deduced by spectroscopy as well as that determined crystallographically for the Rieske center in the bc_1 complex of the respiratory chain (*28*) and in the b_6f complex of chloroplasts (*29*). The crystal structure of NDO has also identified a possible pathway for facilitating electron transfer between the Rieske center of one α-subunit to the mononuclear site of a second α-subunit. Two histidines, an aspartate (bidentate), and a water molecule have been identified as mononuclear-site ligands with a geometry described as "five-coordinated distorted octahedral bipyramid".

The structure and properties of the mononuclear site are considerably less well spectroscopically characterized than the Rieske center, principally because Fe(II) is difficult to access by most spectroscopic tools. In the absence of the substrate, phthalate, Fe(II) can readily be removed from the mononuclear site to yield an apoprotein (apoPDO), while leaving the Rieske center intact. ApoPDO has no capability for catalyzing oxygenations. Addition of 1 mol of Fe(II) per monomer of apoPDO restores full activity. A variety of other divalent metal ions, including Co(II), Cu(II), Mn(II), Ni(II), Cd(II), and Zn(II), can also be bound stoichiometrically to the empty mononuclear site, but only Fe(II) is effective at restoring hydroxylation activity (*14*, *30*). However, small but consistent perturbations of the EPR and visible spectra of the Rieske center are observed upon binding any of the above divalent metal ions (*30*), suggesting that each of these metal ions binds in a similar manner to the mononuclear site.

EXAFS measurements of Fe(II)-, Co(II)-, and Zn(II)-reconstituted PDO have shown that the mononuclear metal ion is ligated exclusively by nitrogen and oxygen donors and that binding of phthalate causes a decrease in the average metal−ligand bond length (*31*). It was suggested that this is consistent with a decrease in coordination number from six to five (*31*). Low-temperature near-IR−MCD measurements have more firmly established this conclusion (*18, 32*). The loss of one mononuclear-site ligand presumably primes the metal center for reaction with O_2. Recent nuclear magnetic relaxation dispersion (NMRD) studies of Cu(II)- and Mn(II)-reconstituted PDO provide evidence that the decrease in coordination effected by phthalate binding is a result of a change in the number of water molecules coordinating the metal ion (*33*). These findings are similar to those for the binding and activation of O_2 at ferrous hemes of cytochromes P450 and related heme oxygenases (*34*), where the binding of substrate displaces a ligand so that O_2 can bind to the iron.

Here we report the results from electronic absorption and EPR spectroscopic studies of the structure and coordination of the mononuclear site of PDO. We have replaced Fe(II) with Cu(II), a spectroscopically more accessible divalent metal ion, to characterize individual coordinating residues. The highly resolved superhyperfine structure observed in the EPR spectra of Cu(II)PDO, selectively labeled with ^{14}N and/or ^{15}N, has allowed the identification of specific ligands that coordinate to the mononuclear metal ion. The results presented herein agree with the crystallographic results for NDO and significantly enhance our knowledge about the active site structure of PDO, which has been a prototype for determining many of the chemical properties of the multicomponent Rieske center-containing nonheme iron dioxygenases.

[2] The strain has previously been referred to as *Pseudomonas cepacia* DB01 but is now classified as belonging to the *Bulkholderia* genus [Yabuuchi, E., Kosako, Y., Oyaiso, H., Yano, I., Hotta, H., Hashimoto, Y., Ezaki, T., and Arakawa,M. (1992) *Microbiol. Immunol. 36*, 1251−1275].

MATERIALS AND METHODS

Enzymes and Chemicals. [^{14}N]PDO and uniformly labeled [^{15}N]PDO [grown on $(^{15}NH_4)_2SO_4$ as the sole nitrogen source] were purified from *B. cepacia* DB01 as described previously by Batie and Ballou (*14*). The histidine auxotroph (*B. cepacia* DB0110) was a gift from Dr. Ronald Olsen (University of Michigan) and was grown as described by Bull and Ballou (*35*), but the medium was supplemented with [δ,ϵ-$^{15}N_2$]histidine. ^{63}Cu was obtained as ^{63}CuO (>99%) from Oak Ridge Laboratories.

Sample Preparation. Substrate was removed from PDO using a Centricon 10 centrifugal concentration tube by repetitive dilution/concentration cycles with 0.1 M HEPES, pH 8.0, containing 0.1 mM dithiothreitol. Fe(II) was then removed from the mononuclear site of PDO (2 mL, 2 mM monomer) by dialysis (three changes of 2 L over 12 h) against 0.1 M HEPES, pH 8.0, containing 0.005 M EDTA. The apoprotein (apoPDO) was exchanged into 0.1 M HEPES, pH 8.0, by dialysis (two changes of 2 L over 12 h). ApoPDO was then passed through a Bio-Rad 10DG desalting column equilibrated with 0.1 M HEPES at pH 8.0 to ensure complete removal of EDTA. Loss of both catalytic activity (as monitored by the rate of decrease in absorbance at 340 nm after NADH and PDR were added) and the characteristic EPR spectrum of reduced apoprotein (see Results) indicated successful removal of Fe(II). Typical activity assays contained 1 μM PDO, 0.2 μM PDR, 2 mM phthalate, 200 μM NADH, and 25 mM Fe(II).

Metal-Reconstituted PDO. ApoPDO was made anaerobic by repetitive gas exchange with argon purified with an Oxiclear oxygen scrubbing cylinder. Reduced Rieske samples were prepared by careful titration with an anaerobic sodium dithionite solution (20 mg/mL, ~0.1 M). Metal ions were reconstituted into the mononuclear site by addition of 1 molar equiv of the divalent metal ion from an anaerobic stock solution (10 mM) to the apoprotein. The forms of the metal ions used were $Fe^{II}(NH_4)_2(SO_4)_2$, $Cu^{II}O$, $Co^{II}Cl_2 \cdot 6H_2O$, $Mn^{II}Cl_2 \cdot 4H_2O$, and $Zn^{II}SO_4 \cdot 7H_2O$. The anaerobic samples were transferred by syringe to an EPR tube that was continuously purged with anaerobic argon, and then they were frozen by slowly immersing the EPR tubes into liquid nitrogen. Oxidized Cu(II)PDO samples were generated by addition of 0.8 molar equiv of natural abundance $Cu^{II}O$ or isotopically enriched $^{63}Cu^{II}O$ to the apoprotein. To contend with the insolubility of copper oxide in aqueous solution, the salt was first dissolved in a minimal volume of 0.1 N HCl and then diluted to the appropriate concentration with deionized water. All samples were prepared in the presence of 5 mM phthalate.

Ferric PDO. ApoPDO was made anaerobic and reconstituted with a nearly stoichiometric (0.95 molar equiv) quantity of Fe(II) from a 10 mM stock solution of $Fe^{II}(NH_4)_2(SO_4)_2$. Fe(II) was oxidized to Fe(III) by titration with $K_3Fe(CN)_6$. Oxidation was assumed to be complete when no further changes were detected in the Fe(III)PDO − Fe(II)PDO difference spectrum.

Spectroscopy. Electronic absorption spectra were measured with a computer-interfaced Perkin-Elmer Lambda 6 UV/vis spectrophotometer employing Perkin-Elmer UV Data Manager software. EPR measurements were made using a Varian Century E-line X-band (9 GHz) EPR spectrometer equipped with a homemade gaseous He flow system to regulate the temperature. The analogue output of each spectrum was recorded digitally on a computer via a data acquisition board made by ComputerBoard Inc. (Mansfield, MA). The specific recording conditions for the EPR spectra are found in the figure captions. The EPR spectra of the spin $^1/_2$ centers were simulated using the *g*-strain programs developed by Hagen et al. (*36, 37*). The spectra for the interacting spin systems were simulated using a *g*-strain-adapted version of the spin−spin interaction program (*38, 39*).

RESULTS

Several different divalent metal ions can be bound individually in the mononuclear site of PDO, as mentioned above (*14*). We chose Cu(II) as a spectroscopic probe of the mononuclear site because it has narrow EPR lines that are useful for examining for the presence of nitrogenous ligands. However, to ensure that Cu(II) as a probe would provide information relevant to catalysis, it was necessary to ascertain whether Cu(II) and other divalent metal ions bind in substantially the same way as does Fe(II). Described below are several spectroscopic experiments that establish this premise.

Effects of Metal Ion Binding on the Rieske Center. The oxidized Rieske [2Fe-2S] center, like other [2Fe-2S] centers, has two high-spin (d^5) Fe(III) ions that are antiferromagnetically spin-coupled to yield a ground state with $S = 0$. Thus, there is no low-temperature EPR signal (*40*). When the Rieske center is reduced by one electron, the Fe(III) high-spin (d^5)−Fe(II) high-spin (d^6) pair is valence-trapped and coupled to form a ground state with a net spin of $^1/_2$. The EPR spectrum of reduced apoPDO at 25 K shown in Figure 1A is that of a classical Rieske center with *g*-values at 2.007, 1.904, and 1.758 ($g_{av} = 1.89$) (*19*); i.e., it exhibits a very low g_{av} in comparison with other [2Fe-2S] centers. When 1 molar equiv of Fe(II) is added to such a reduced apoPDO sample, the EPR spectrum shown in Figure 1B is obtained. A small change in g_1 and g_2 (numbering from left to right on the spectrum) and a large change in g_3 accompany the binding of Fe(II) to the cofactor iron site. Note that there is no direct EPR contribution from the cofactor iron site, because the iron is ferrous, which is usually EPR-silent. The Gibson model for [2Fe-2S] centers (*41*) associates a change in g_3 with a change in the crystal field splitting, specifically Δ_{yz}, at the ferrous atom. Therefore, we assume that occupancy of the cofactor iron site causes a subtle change at the ferrous ion in the reduced [2Fe-2S] cluster. The change must be subtle, because g_1 and g_2 of the [2Fe-2S] cluster are essentially unchanged by this occupancy. A titration of the g_1 line width of the Rieske center as a function of the Fe(II) present per PDO monomer (Figure 2) shows that 1 equiv of Fe(II) binds tightly to each monomer, confirming that this binding is specific to a single site.

Remarkably, when the mononuclear site is populated with either paramagnetic metal ions [Fe(II), Cu(II), or Mn(II), Figure 1B−D] or diamagnetic metal ions [e.g., Zn(II), Figure 1E], the EPR parameters (Table 1) of the spectra of the reduced iron−sulfur center are changed from that of the apoprotein in essentially the same manner. (The contributions both from the perturbed Rieske center and from the bound metal ion can be deconvoluted. The bound metal ion

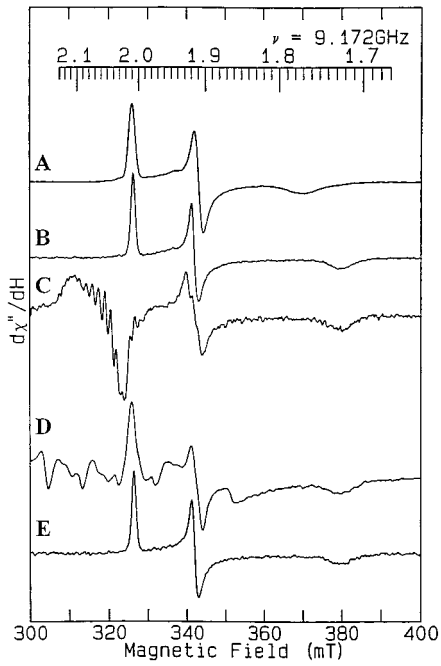

FIGURE 1: X-band EPR spectra at 25 K of reduced forms of PDO. Samples were reduced with 10 mM sodium dithionite under argon gas. Metal-reconstituted samples were prepared by the addition of 1.1 molar equiv of the appropriate metal salt in the presence of 5 mM phthalate. Curves: (A) apoPDO, (B) Fe(II)-reconstituted PDO, (C) Cu(II)-reconstituted PDO, (D) Mn(II)-reconstituted PDO, and (E) Zn(II)-reconstituted PDO. Proteins were 300 μM (based on the Rieske center or monomer concentrations). EPR conditions: microwave frequency, 9.173 GHz; microwave power, 0.2 mW; and modulation amplitude, 5 G.

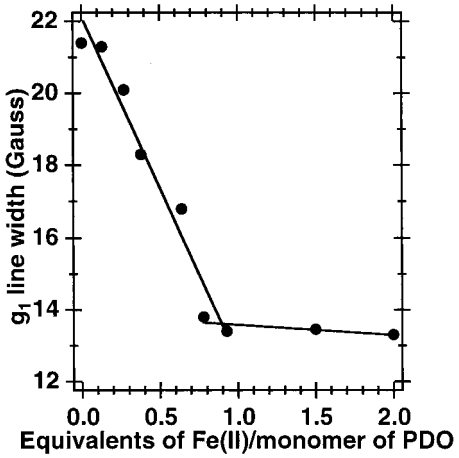

FIGURE 2: Plot of the EPR g_1 resonance line width at half-height of the reduced Rieske center as a function of added Fe(II). The PDO concentration was 176 μM. EPR conditions: temperature, 20 K; microwave frequency, 9.226 GHz; microwave power, 0.2 mW; and modulation amplitude, 10 G.

contributions can be determined from EPR spectra of the sample when the Rieske center is oxidized and thereby has no spectral contributions.) Thus, the high-field shift of g_3 cannot be a result of a magnetic interaction between paramagnetic centers; rather, it more likely is due to the ligation at the mononuclear site transmitting conformational effects to the ligands of the Fe(II) of the [2Fe-2S] center.

When a paramagnetic ion such as Cu(II) or Mn(II) binds to the mononuclear site, it can be predicted that there will be interactions with the paramagnetic reduced Rieske center, unless the distances are too great or some other special

Table 1: EPR Parameters for the Reduced Rieske Center in the Absence or Presence of Divalent Metal Ions at the Mononuclear Site[a]

g-value (G)	apo-PDO (no metal)	Fe(II)[b]	Cu(II)[b]	Mn(II)[b]	Zn(II)[b]
g_1	2.007	2.005	−[c]	2.008	2.005
g_2	1.904	1.911	1.907	1.908	1.911
g_3	1.758	1.717	1.714	1.720	1.718

[a] All samples contained 5 mM phthalate. (See legend to Figure 2 for experimental conditions). [b] Generated by the addition of 1.1 molar equiv of the appropriate metal to apoPDO. [c] Not determined due to interference from the $g_\perp$ resonance of Cu(II).

condition applies. Such interactions usually occur either via spin exchange (electrostatic) or dipolar (magnetic) coupling. They can be grouped into two main categories: those where the exchange interaction is much smaller than the energy of the microwave quantum ($\sim$0.3 cm^{-1} at X-band EPR) and those where the exchange interaction results in a true coupling of the spin systems to produce a triplet ($S = 1$) system. [This would be true in the case where Cu(II) is used; an $S = 2$ or 3 state would result from the addition of Mn(II).] The triplet system is not appropriate for consideration in PDO, because the size of the exchange interaction is too small (*42*). If the magnetic interaction were sufficiently large, and if it were between two spin systems that did not align with the applied field (i.e., the spin systems have anisotropic g-tensors), then there would be a half-field resonance at $g = 4$ that is due to the magnetic dipole−dipole interaction. The magnitude of this class of resonance is proportional to $1/r^6$ and also depends on resonances that are not along the principal axis of the g-tensors; therefore, it is difficult to predict its intensity (or presence) without a computer simulation to the data. The absence of a $g = 4$ resonance at the sensitivity limit of the spectrometer prevents meaningful calculation of a minimum distance between the two paramagnetic centers. Therefore, to estimate the interaction of Cu(II) and the Rieske center, we compared the line width of the cupric EPR signal at 25 and 130 K. At 130 K the EPR signal of the Rieske center in reduced Cu(II)PDO is not observable because the increased spin relaxation rate causes the magnetic field from the Rieske center to be time averaged to zero. This allows us to observe the cupric signal with the same sample. The line width of the z-component of the cupric signal is 3.2 mT at fwhm at both 25 and 130 K (data not shown). Therefore, no interaction between the Rieske center and cupric ion could be discerned. A 10% EPR change in line width (0.32 mT) would be easily detected. Using the rule that the dipolar interaction between two $S = {}^1/_2$ systems is 1 mT at 10 Å distance and that the interaction depends on $1/d$ (d = distance),[3] we calculate that a 15 Å center-to-center distance would correspond to an interaction size of 0.32 mT. Therefore, we believe that we would have seen the interaction signal as a broadening of the EPR signal, if the distance between the Rieske center and Cu(II) were significantly smaller than 15 Å.

The UV−visible absorption spectrum of oxidized apoPDO is dominated by the Rieske center chromophore, and it, like the EPR spectrum, is slightly perturbed (1−5% increases in the molar absorbance of the 460 nm band) on binding divalent metal ions. The measured perturbations are very similar for each of the metal ions used [Fe(II), Co(II), Cu(II),

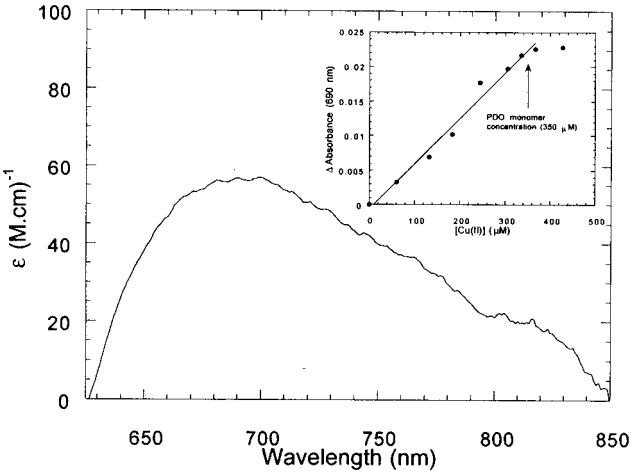

FIGURE 3: Visible difference spectrum of phthalate-bound Cu(II)-reconstituted PDO−phthalate-bound Fe(II)-reconstituted PDO. Inset: titration of apoPDO with Cu(II) monitored as the change in absorbance at 690 nm. The protein concentration was 350 μM monomer. The phthalate concentration was 5 mM.

Mn(II), Ni(II), Cd(II), and Zn(II)], and titrations reveal a 1:1 binding stoichiometry with K_d values less than 1 mM for each of the metal ions (*30, 43*). Fe(II) binds with a K_d of less than 1 μM (*14*). Cu(II) binds less tightly to PDO than does either Fe(II) or Co(II). In the presence of substrate, the binding of each of these metal ions becomes 10^3-10^4-fold tighter, suggesting that the binding is similar for each of the metal ions (*43*). Although these phenomena parallel the results of the EPR experiments on the reduced enzyme, we cannot be sure that the perturbations observed in the optical spectra of the oxidized Rieske center are due to the same factors as those that modulate the EPR spectra of the reduced Rieske center; the oxidized form of the Rieske center does not exhibit any EPR signal so that direct comparisons are not possible.

The UV−visible spectra of the Fe(II)- and Cu(II)-reconstituted proteins are nearly indistinguishable from each other principally because the Rieske center is the dominating chromophore. However, subtraction of the spectrum of the substrate-bound form of Fe(II)PDO from that of the substrate-bound Cu(II)PDO (Figure 3) largely cancels the spectroscopic changes to the Rieske center that are due to substrate and metal ion binding. Thus, any weak transitions that result from the direct metal−protein interactions are emphasized. This subtraction reveals an additional low intensity d−d transition centered at ~690 nm ($\epsilon = 58$ M^{-1} cm^{-1}) that is comparable to the weak spin-forbidden transitions observed in the naturally occurring type 2 or "normal" copper sites in copper proteins and also in Cu(II)-reconstituted isopenicillin *N*-synthase (*44, 45*). Ferrous d−d interactions are very weak and therefore do not have significant optical contributions. Comparison of this difference spectrum to those of synthetic copper complexes suggests that the observed transition can be attributed to either five- or six-coordinate Cu(II) (*46*). In light of considerable spectroscopic evidence supporting a decrease in coordination number upon substrate binding (*18, 32, 33*), the presence of phthalate in this sample suggests that the observed transition most likely indicates a five-coordinate configuration. The absorbance at 690 nm was observed to increase linearly as Cu(II) was titrated into the apoprotein (inset Figure 3), and no further increase at 690 nm was observed after the addition of ~1.1 equiv of Cu(II). This suggests that each monomer of the protein binds ~1 Cu(II) atom in a specific manner, presumably in nearly the same way that it binds Fe(II).

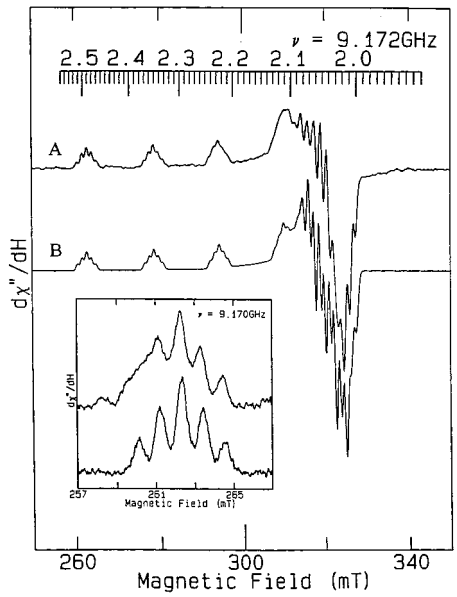

FIGURE 4: (A) X-band EPR spectrum at 120 K of ^{63}Cu(II)-reconstituted PDO (200 μM monomer) with natural abundance nitrogen (^{14}N ~98%) in the presence of 5 mM phthalate. EPR conditions: microwave frequency, 9.172 GHz; microwave power, 2 mW; and modulation amplitude, 5 G. Inset: EPR spectra of the lowest field resonance (~263 mT) for natural abundance Cu(II)-reconstituted (200 μM monomer, top spectrum) and ^{63}Cu(II)-reconstituted [^{14}N]PDO (200 μM monomer, lower spectrum). EPR conditions were the same as in the main figure, with the exception that the power used for recording the upper spectrum (inset) was 20 mW (a power level that does not saturate the EPR signal). (B) Simulation of the spectrum using the parameters in Table 2.

Overall, the above studies show that several different divalent metal ions can be individually incorporated into the mononuclear site in place of iron, although only Fe(II) is competent for regenerating enzymatic dioxygenation properties (other properties, including enhancement of substrate binding and stimulation of the rate of electron transfer to the Rieske center, will be discussed in a future communication). The other metal ions appear to bind very similarly to Fe(II); they bind with 1:1 stoichiometry, their binding is enhanced by the presence of substrate, and they affect both the EPR and visible properties of the distant Rieske center very nearly identically. These similar properties provide a basis for considering that the use of a paramagnetic divalent metal ion such as Cu(II) to probe the nature of the mononuclear site is likely to provide relevant information about the natural enzyme.

EPR of Cu(II)-Reconstituted Oxidized ApoPDO. Cu(II) bound to oxidized PDO can serve as a paramagnetic probe of the mononuclear site, and because the oxidized Rieske center has a ground-state spin of 0, it will not interfere with the copper EPR spectrum. Naturally abundant copper consists of two isotopes (^{63}Cu ~70% and ^{65}Cu ~30%), both with nuclear spin $I = {}^3/_2$ but with slightly different magnetic moments; thus, the spectra due to the two isotopes will be very similar, but the *g*-values will be slightly different. The EPR spectrum of apoPDO reconstituted with ^{63}Cu (Figure 4) has a four-line hyperfine pattern (with peaks at $g = 2.49$,

Table 2: EPR Parameters for Cu(II)-Reconstituted PDO[a]

	Cu(II)PDO sample[b,c]		
parameter	[^{14}N]PDO	[^{15}N]PDO	[$^{15}N_2$]His−PDO
$g_\perp$	2.053	2.053	2.068
$g_\parallel$	2.285	2.285	2.326
$A_\perp$	14	14	15
$A_\parallel$	168	168	153
A_N	11.4	16	16

[a] See legends to Figures 3−5 for experimental details. [b] All samples contained 5 mM phthalate. [c] Generated by the addition of 0.8 molar equiv of ^{63}Cu(II). *g*-values and *A*-values (hyperfine constants) are presented in units of gauss. The nitrogen hyperfine tensor is assumed to be isotropic.

Scheme 2: Splitting Patterns for Nitrogen

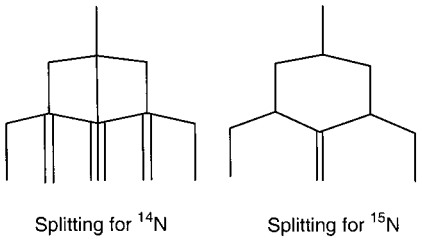

2.35, 2.22, and 2.11) and shows highly resolved superhyperfine interactions. This is similar to a variety of proteins containing tetragonal type 2 Cu(II) sites and is also consistent with the UV−visible data discussed above. The simulated EPR spectrum, labeled B in Figure 4, fits the experimental data reasonably well. EPR parameters used for this fit are given in Table 2.

The resonance at lowest field (centered at ~262 mT; g = 2.49) demonstrates a highly resolved superhyperfine pattern of five peaks with relative intensities 1:2:3:2:1 (inset, Figure 4). Nitrogen is the most common nucleus giving rise to such superhyperfine structure, and because ^{14}N accounts for ~98% of the naturally abundant element, effects from other nitrogen isotopes are negligible. The nuclear spin (I) of ^{14}N is 1, so that each equivalent ^{14}N nucleus splits the EPR of copper into three equally intense peaks. Thus, the observed five-line pattern can be attributed to two equivalent nitrogen nuclei [$2(n)I + 1 = 5$, where n is the number of coordinating nitrogen nuclei and I is the nuclear spin of ^{14}N]. See Scheme 2. Initial studies that employed natural abundance $^{63/65}$Cu(II) also exhibited a complex hyperfine pattern, but the low-field region was not as well resolved (inset to Figure 4), due to spectral overlap from the slightly different magnetic moments of the two isotopes. This demonstrates the value of using a homogeneous isotope.

To eliminate the possibility that the spectra in Figure 4 were due to adventitiously bound copper, we deliberately prepared a sample that contained adventitiously bound copper and measured its spectrum. ^{63}Cu(II) (0.8 equiv) was added to a sample that previously had been reconstituted with Fe(II) in the presence of substrate. ApoPDO binds Fe(II) with a K_d <1 μM (*30*); in the presence of substrate it binds metal ions approximately 1000-fold more tightly (*43*). ApoPDO binds Cu(II) almost 1000-fold less tightly than it does Fe(II) (*43*). This ensured that Fe(II) would not be displaced from the mononuclear site by Cu(II). Thus, any copper that was bound to PDO would not be at the mononuclear site. The EPR spectrum of this sample was significantly different from

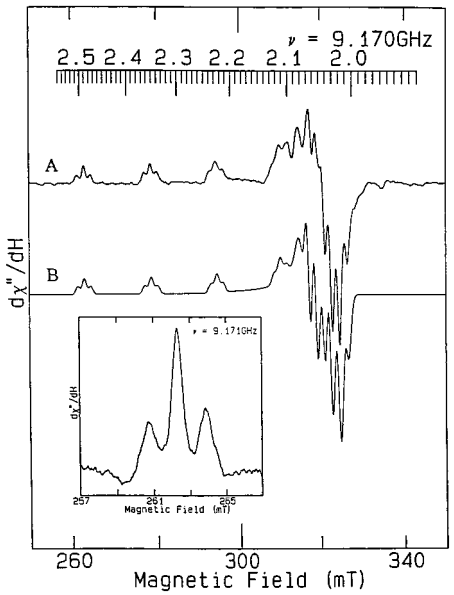

FIGURE 5: (A) X-band EPR spectrum at 120 K of ^{63}Cu(II)-reconstituted PDO (200 μM monomer), which was prepared from cells grown on $(^{15}NH_4)_2SO_4$. EPR conditions were the same as in Figure 4. Inset: EPR spectra of the lowest field resonance (~263 mT) of ^{63}Cu(II)-reconstituted [^{15}N]PDO (200 μM monomer). (B) Simulation of the EPR spectrum using the parameters in Table 2.

that of Cu(II)-reconstituted apoPDO. Parameters for the adventitiously bound copper were $g_\parallel$ = 2.225, $g_\perp$ = 2.048, $A_\parallel$ = 178, and $A_\perp$ = 16. This compares with the values of $g_\parallel$ = 2.285, $g_\perp$ = 2.053, $A_\parallel$ 168, and $A_\perp$ = 14 for ^{63}Cu(II) to the mononuclear site. Thus, it can be concluded that the spectra in Figure 4 were of Cu(II) bound to the mononuclear site.

Another experiment to verify that the superhyperfine splitting is due to two nitrogens used ^{15}N-labeled PDO. For these experiments, PDO was isolated from *B. cepacia* grown on isotopically enriched [^{15}N]ammonium sulfate as a nitrogen source, and this provided PDO that was uniformly labeled with ^{15}N ([^{15}N]PDO). If the copper is ligated to two nitrogens, the ^{15}N, which has a nuclear spin of $^1/_2$, should yield predictable changes in the EPR spectrum (see Scheme 2). The EPR spectrum (Figure 5) was again typical of type 2 copper, and could be simulated with values of $g_\perp$, $g_\parallel$, $A_\perp$, and $A_\parallel$ identical to those used for [^{14}N]PDO (Table 2). The low-field resonance consisted of three highly resolved superhyperfine peaks of relative intensities 1:2:1, consistent with splitting by two equivalent ^{15}N nuclei (inset, Figure 5). The only significant difference in the observed EPR parameters was an increase in the value of A_N (Table 2), which is proportional to the nuclear *g*-value. The ratio of the hyperfine splittings (A_N) of ^{14}N (11.4 G) to that of ^{15}N (16 G) (Table 2) is in good agreement with the ratio of the respective nuclear magnetic moments divided by the spin of the nitrogens, confirming that copper in both samples resides in identical environments. These results establish the presence of two nitrogen ligands coordinating to the Cu(II).

We prepared a sample in which the only ^{15}N-labeling was in histidine by growing a histidine auxotroph (*B. cepacia* DB101) on uniformly labeled [^{15}N]histidine with natural abundance ammonium sulfate as a nitrogen source (*22*). The EPR spectrum of PDO isolated from this histidine auxotroph grown on [δ,ϵ-$^{15}N_2$]histidine and reconstituted with ^{63}Cu(II)

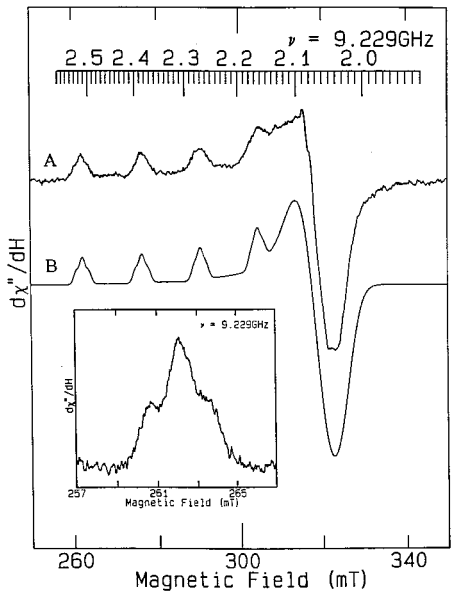

FIGURE 6: (A) X-band EPR spectrum at 120 K of ^{63}Cu(II)-reconstituted PDO (200 μM monomer) in which all histidine nitrogens are ^{15}N and all protein nitrogens are ^{14}N. EPR conditions: microwave frequency, 9.226 GHz; microwave power, 0.5 mW; and modulation amplitude, 10 G. (B) Simulation of the EPR spectrum using the parameters in Table 2.

([$^{15}N_2$]His-PDO]) could clearly be attributed to type 2 copper Figure 6. The lowest field resonance was shown to exhibit a three-line pattern similar to that of [^{15}N]PDO (inset, Figure 6, but was considerably less well resolved. The poorer resolution was attributed to insufficient (or absence of) phthalate and possibly to a slight excess of copper. The *g*-values (Table 2) are somewhat different from those of the other samples and are typical of Cu(II)PDO in the absence of substrate. A similarly poorly resolved spectrum of [^{14}N]-PDO (not shown) was converted to a highly resolved spectrum identical to that in Figure 4 by removal of Cu(II) and reconstitution with a slightly substoichiometric amount of ^{63}Cu(II) in the presence of excess phthalate. The same procedure could not be performed on the [$^{15}N_2$]His-PDO sample because of limited quantities of protein.

Properties of Fe(III)-Substituted PDO. We have prepared Fe(III)PDO in an attempt to quantify histidine and/or tyrosine ligation at the mononuclear site when a metal ion more like the native Fe(II) than is Cu(II) is present. Fe(III) is more spectroscopically accessible than is Fe(II), and iron coordination spheres are not significantly altered in going between the ferric and ferrous oxidation states. Furthermore, iron can be found in a variety of coordination environments and does not display significant redox geometrical preferences, in contrast to Cu(II). Fe(III)PDO could not be generated from apoPDO by directly adding Fe(III) to apoPDO, presumably due to the insolubility of Fe(III) in aqueous solution. However, it could be generated by oxidizing Fe(II)-reconstituted PDO with 1 molar equiv of potassium ferricyanide. In the presence of PDR, such ferric samples did catalyze NADH oxidation and generated dihydrodiol product, but the maximum activity was only 50% that of protein reconstituted with Fe(II). The activity observed with the ferric sample was presumably brought about by the Fe(III) first being reduced to Fe(II) by the reductase (PDR), so that under these conditions ~50% of the sample participated as native enzyme. Fe(III)PDO did not exhibit any iron−tyrosinate charge-transfer bands, implying that there is no ligation by tyrosine at the active site. The only resonance observed in the low-temperature EPR spectrum of the latter sample was a $g = 4.3$ signal, which is often associated with adventitiously bound high-spin Fe(III).

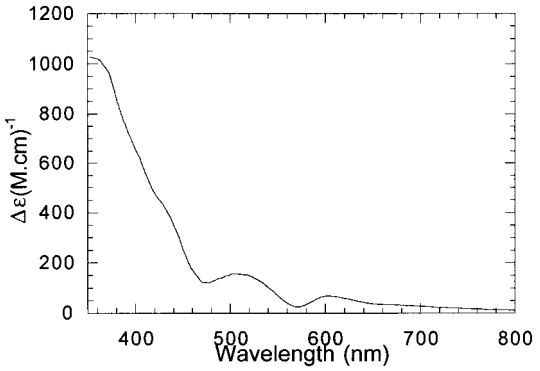

FIGURE 7: Electronic absorption difference spectrum at 25 °C of the phthalate-bound forms of Fe(III)PDO−Fe(II)PDO. Fe(III)PDO was generated as described in Materials and Methods. The protein concentration was 80 μM monomer.

The difference of the spectrum obtained by subtracting that of Fe(II)PDO from that of Fe(III)PDO has significant intensity (~1000 $M^{-1}cm^{-1}$) near 350 nm (Figure 7). Similar absorbance at this wavelength has been attributed to Fe(III)−His ligand-to-metal charge-transfer transitions in other non-heme iron-containing proteins (*47*). The ferric adducts of superoxide dismutase (*48*) and lipoxygenase (*49*) show increases of ~1800 M^{-1} cm^{-1}. The iron in both of these proteins has been shown to be coordinated by three histidines. The corresponding ferric-containing phenylalanine and tyrosine hydroxylases are coordinated by two histidines (*50*, *51*) and exhibit an increase around 350 nm of about 1000 M^{-1} cm^{-1} (*52*), similar to that of PDO. To the extent that the intensity at ~350 nm correlates with the number of histidines coordinating Fe(III), these results are consistent with the coordination in Fe(III)PDO involving two histidines, like that of tyrosine and phenylalanine hydroxylases. These optical studies also correlate with the EPR results obtained for Cu(II)PDO (above).

Protocatechuate dioxygenase, which contains a ferric mononuclear site that is ligated by two tyrosines and two histidines (*53*, *54*), has a deep burgundy color associated with the intense Fe(III)−Tyr bands and exhibits an $\epsilon_{460nm} \sim 3500$ M^{-1} cm^{-1} (*35*). Since there are no intense Fe(III)−Tyr transitions with the Fe(III)-substituted PDO, it is unlikely that tyrosine ligation occurs at the mononuclear site of PDO.

DISCUSSION

Interaction of the Mononuclear Metal Ion with the Rieske Center. Gassner has shown that metal ion binding to PDO affects a range of its properties (*43*). An increase in the affinity for phthalate, an enhancement in the rate of intermolecular electron transfer from the reductase protein, and decreases in the midpoint redox potential of the Rieske center all resulted from adding metal ion to the mononuclear site. The nature of these complex changes is unclear, but it is curious that two sites ≥12−15 Å (see Results and ref *27*) can affect each other so significantly. Studies by ENDOR and resonance Raman spectroscopies have shown there to

be no change in the metal−ligand distance within the Rieske cluster when metal ion binds to the mononuclear site (*21*−*25*). This concurs with results reported here that show the g_{av} values are changed only slightly in going from apo- to metal-reconstituted PDO; changes that affect the electronic nature of Rieske ligands are known to result in significant changes in g_{av} (*55*). Although we do not know how metal ion that binds at a site 12−15 Å away causes these small changes in the geometry of the Rieske cluster, this work indicates (no interaction signals) that it is not the result of direct electronic interactions. Therefore, the most plausible explanation appears to be that the metal-binding effects occur through interactions with its ligands. The X-ray structure of NDO indicates that Asp-205 [corresponding to Asp-189 in PDO numbering (*56*)] is hydrogen-bonded across the α-subunit interface to both His-104 (corresponding to His-92 in PDO) of the Rieske center and His-208 (His-181 of PDO) of the mononuclear site. If such a network is present in PDO, it may explain how structural changes associated with metal ion binding at the mononuclear site may be conveyed to a Rieske center of an adjacent α-subunit. Whatever the cause, it appears that the effects of the bound metal ion on the spectroscopic properties of the Rieske center correlate with the decrease in its midpoint reduction potential and the increased rate of electron transfer from PDR. Furthermore, this same conformational event may explain the increased affinity of the mononuclear site for substrate caused by the binding of metal ion. The results with PDO can be compared with earlier EPR studies of putidamonoxin [PMO, a Rieske mononuclear Fe(II)-containing monooxygenase that catalyzes the O-demethylation of 4-methoxybenzoate], which reported *g*-values for the reduced Rieske center of $g_1 = 2.010$, $g_2 = 1.910$, and $g_3 = 1.780$ (*57*), similar to the values for apoPDO shown in Table 2. Examination of the EPR spectrum of PMO shows a complex spectrum that likely is a mixture of both metal-bound and apoPMO species. In subsequent EPR studies the *g*-values were reevaluated to be $g_1 = 2.008$, $g_2 = 1.913$, and $g_3 = 1.720$ (*58*), which are consistent with those for PDO. The reasons for this change were not addressed, but it appears possible that early protein preparations contained substoichiometric quantities of Fe(II) at the mononuclear site. Thus, the binding of Fe(II) may cause similar conformational effects on the [2Fe-2S] centers in two distinct Rieske non-heme iron oxygenases that catalyze significantly different reactions. It will be interesting to see whether the Rieske and the mononuclear sites are in similar positions relative to one another in both proteins and whether the protein milieu between the two sites is also similar.

Cu(II) as a Paramagnetic Probe of the Mononuclear Site. Perturbations in the EPR spectra of the reduced Rieske center suggest that Cu(II) binds to apoPDO at the same site and in a manner similar to that of Fe(II). Cu(II) has previously been used to probe the coordination spheres of a variety of naturally occurring Zn(II) proteins, including carbonic anhydrase (*59*, *60*), alkaline phosphatase (*61*), and superoxide dismutase (*62*), and Fe(II)-containing proteins, including phenylalanine hydroxylase (*63*) and isopenicillin N synthase (*45*, *64*). The early studies on Cu(II)-reconstituted zinc proteins were particularly successful in identifying coordinating histidine residues by virtue of their well-resolved superhyperfine structure, especially when reconstituted with ^{63}Cu. In contrast, reconstitution with Cu(II) of proteins normally containing Fe(II) revealed insufficiently resolved superhyperfine splitting to assign coordinating ligands. However, ESEEM spectroscopic studies of Cu(II)-reconstituted forms of phenylalanine hydroxylase (including histidine mutants) (*63*) and isopenicillin N synthase (*64*) were successful in identifying coordinating histidine residues. In the present study, we observe unusually well-resolved superhyperfine structure in the Cu(II)-reconstituted PDO. Comparison of the corresponding EPR spectra of uniformly labeled [^{14}N]- and [^{15}N]PDO shows that all the features are reproduced in each spectrum, and these results provide conclusive evidence for two nitrogenous ligands. The EPR results with [$^{15}N_2$]His-PDO show that the nitrogenous ligands are histidines.

Scheme 3

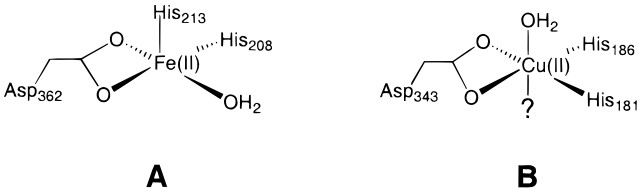

A **B**

Role of Tyrosine at the Mononuclear Site. Comparisons of the amino acid sequences for a series of Rieske oxygenases that catalyze the formation of *cis*-dihydrodiols have identified several highly conserved amino acids, including those bearing carboxylates, a tyrosine, and two histidines within a consensus sequence (**E**$X_{3/4}$**D**X(**Y**)**H**$X_{4/5}$**H**), as well as another tyrosine and an aspartate about 150 residues downstream (*56*, *65*−*67*). (The tyrosine in the consensus sequence above is not present in PDO, but other tyrosines are present downstream.) Mutagenesis of the corresponding Asp, Glu, and His residues to alanines in toluene dioxygenase resulted in a total loss of activity, while Tyr to Ala mutants retained partial activity (*66*). A complementary study of benzene dioxygenase also found that mutation of the corresponding tyrosine residues to alanines results in considerable, but incomplete loss of activity (*68*). The absence of Fe(III)−Tyr transitions in the optical spectrum of Fe(III)PDO and the above-mentioned mutational studies are all consistent with tyrosine participating in catalysis but not as a mononuclear metal ion ligand.

Structural Implications. A cartoon, adapted from the recent crystal structure (*27*), depicting the mononuclear site of NDO is presented in Scheme 3A. Crystal structures have also been determined for six other non-heme iron [Fe(II)]-containing proteins that react with oxygen, including lipoxygenase (*69*, *70*), 2,3-dihydroxybiphenyl 1,2-dioxygenase (*71*, *72*), tyrosine hydroxylase (*51*), phenylalanine hydroxylase (*50*), Mn(II)-reconstituted and Fe(II)-substrate bound forms of isopenicillin N synthase (*73*), and cephalosporin synthase (*74*, *75*). The structures of these and of NDO are all very similar and suggest that many mononuclear Fe(II)-containing enzymes employ a general structural theme. The non-heme Fe(II) in each of the above structures is coordinated by histidines, carboxylate, and solvent-derived water, and has been reviewed recently (*76*). These structures all show a triad of the two histidines and a carboxylate anchoring the Fe(II) and permitting up to three additional ligands at the free sites (*76*). Like PDO, the Fe(II) sites in each of these proteins exhibit no EPR spectra and are essentially colorless. By

contrast, Fe(III)-containing protocatechuate 3,4-dioxygenase, for which structures are also available (*53*, *54*), is coordinated by two histidines and two tyrosines and does exhibit both visible color and an EPR spectrum. A combination of our present findings with those of previous spectroscopic studies, available crystallographic data, and comparison of PDO and NDO amino acid sequences suggests the structure for the mononuclear site depicted in Scheme 3B for PDO in the absence of substrate. As shown, the mononuclear site in NDO is very similar to that postulated for PDO in Scheme 3. The hypothesis that the **H**X_{4-5}**H** motif contains the ligating histidines in PDO and other Rieske oxygenases (*65*) has been verified in the structures of NDO (His-208 and His-213) (*27*), lipoxygenase (His-499 and His-504) (*69, 70*), tyrosine hydroxylase (His-331 and His-336) (*51*), and phenylalanine hydroxylase (His-286 and His-291) (*50*). In each of these proteins, one histidine is axially coordinated while the other binds equatorially, and together they form a 2-His−1-carboxylate facial triad (*76*). The EPR studies described here on the Cu(II)-substituted PDO have identified two metal-coordinating histidines. Because these two residues appear to be spectroscopically equivalent, and the $g_{||}$ and $A_{||}$ values (Table 2) imply that the complex is square pyramidal, we have positioned both equatorially. In contrast to the reported NDO structure, perhaps because of the characteristics of copper, PDO may bind copper equidistantly between the two histidines, thus defining the equatorial plane. This could occur with only a slight distortion of the ligand environment (Scheme 3).

Water coordination of Cu(II)PDO, as determined using proton relaxation methods (*33*), has identified one coordinating water molecule when substrate is present and suggests the presence of a second water when substrate is absent. MCD (*18*,*32*) and EXAFS (*31*) studies have shown that one ligand is lost upon substrate binding. Thus, it is possible that two water molecules are actually ligated in the substrate-free form, one of them exhibiting proton relaxation times too long to be detected (or is bound so tightly that it does not exchange sufficiently fast with bulk solvent to contribute significantly to the overall observed relaxation). When phthalate is bound, the less tightly bound water moves farther away from the metal ion, suggesting that the ligand displaced in the presence of phthalate is a coordinated water. The second water then becomes detectable. Since measurements reported here were all in the presence of high concentrations of phthalate, which would force the removal of the dissociable ligand, it is clear that histidine is not the dissociable ligand. This is in accordance with the postulates of Hegg and Que for the properties of the mononuclear Fe(II) oxygenases (*76*). The structure shown in Scheme 3B represents the substrate-free site.

While it is likely that substitution of Cu(II) for Fe(II) will affect the coordination geometry of the mononuclear site, compelling spectroscopic evidence (*18, 31, 32*) supporting a six-coordinate substrate-free site in native enzyme has prompted us to include a sixth ligand, denoted as "?", in our model for the native site. No experimental evidence is available regarding the identity of this ligand; however, by analogy to other crystallographically characterized mononuclear Fe(II) sites (*4, 76*), a second water molecule, a third histidine, or an amide ligand derived from a Gln or Asn residue is a likely candidate. This last type of coordination has been observed for lipoxygenase (*69, 77*) and isopenicillin N synthase (*73, 75*), and has been suggested for NDO. However, because in NDO Asn-201 is 3.7 Å away from Fe(II), it is too distant to ligate to the Fe(II). Moreover, while a residue corresponding to Asn-201 of NDO is conserved in a majority of aromatic ring dioxygenases, it is apparently absent from others, including PDO.

NDO has an $\alpha_3\beta_3$ mushroom-shaped structure. The distance from the Rieske center to the mononuclear iron in a single subunit is 43.5 Å, which would be extremely long for efficient electron transfer. However, the distance from the Rieske center of one subunit to the mononuclear iron in the adjacent subunit is only about 12 Å, and it is hypothesized that electron transfer in catalysis actually takes place between subunits (*27*). If in PDO the distance were also 12 Å or greater, it would account for the lack of observable paramagnetic interactions between the mononuclear site and the Rieske center reported in this work for PDO. It will be interesting to find out if PDO has a similar overall structure to NDO.

CONCLUSION

Detailed knowledge of the Fe(II) mononuclear site structure is very important for the elucidation of the mechanism for the cis-dihydroxylation reactions of bacterial dioxygenases. The identification by EPR spectroscopy of two histidines coordinating at the mononuclear metal ion of PDO represents the only specific ligand information available for PDO, and this correlates beautifully with the crystal structure of NDO (*27*). We have recently reported ^{19}F NMR relaxation studies that show how F-phthalates (substrate) are positioned optimally in the active site to allow the Fe(II) to activate oxygen and bring about the cis-dihydroxylation reaction (*78*). As discussed above, binding presumably occurs in concert with the release of a water ligand. Overall, these and other studies (*18, 31*−*33*) indicate the importance of changes of ligation that occur during catalysis. The flexible coordination to Fe(II) in these enzymes is likely to be crucial for these oxygenative events (*76*). The results from these studies provide excellent examples of the use of spectroscopic techniques to elucidate molecular structures in the native state. Similarities in the primary structures and the specificity of the reactions catalyzed (e.g., to form *cis*-dihydrodiols) suggest that PDO is representative of all of the Rieske oxygenases and that the results of this study should be applicable to many other systems.

ACKNOWLEDGMENT

We thank George Gassner for supplying enzyme samples and James Penner-Hahn for review of the manuscript.

REFERENCES

1. Gibson, D. T. (1971) *Crit. Rev. Microbiol. 1*, 199−223.
2. Wood, J. M. (1982) *Environ. Sci. Technol.* 291a−297a.
3. Mason, J. R., and Cammack, R. (1992) *Annu. Rev. Microbiol. 46*, 277−305.
4. Que, L., and Ho, R. Y. N. (1996) *Chem. Rev. 96*, 2607−2624.
5. Gibson, D. T., Koch, J. R., and Kallio, R. E. (1968) *Biochemistry 7*, 2653−2662.
6. Reiner, A. M. (1971) *J. Bacteriol. 108*, 89−94.

7. Gibson, D. T., Hensley, M., Yoshioka, H., and Mabry, T. J. (1970) *Biochemistry 9*, 1626−1630.
8. Jeffery, A. M., Yeh, H. J. C., Jerina, D. M., Patel, T. R., Davey, J. F., and Gibson, D. T. (1975) *Biochemistry 14*, 575−583.
9. Keyser, P., Pujar, B. G., Eaton, R. W., and Ribbons, D. W. (1976) *Environ. Health Perspect.* 159−166.
10. Pujar, B. G., and Ribbons, D. W. (1985) *Appl. Environ. Microbiol. 49*, 374−376.
11. Nomura, Y., Harashima, S., and Oshima, Y. (1989) *J. Ferment. Bioeng. 67*, 291−296.
12. Nakazawa, T., and Hayashi, E. (1977) *J. Bacteriol. 131*, 42−48.
13. Nomura, Y., Takada, N., and Oshima, Y. (1989) *J. Ferment. Bioeng. 67*, 297−299.
14. Batie, C. J., LaHaie, E., and Ballou, D. P. (1987) *J. Biol. Chem. 262*, 1510−1518.
15. Correll, C. C., Batie, C. J., Ballou, D. P., and Ludwig, M. L. (1992) *Science 258*, 1604−1610.
16. Gassner, G. T., Ludwig, M. L., Gatti, D. L., Correll, C. C., and Ballou, D. P. (1995) *FASEB J. 9*, 1411−1418.
17. Batie, C. J., Ballou, D. P., and Correll, C. C. (1992) in *Chemistry and Biochemistry of Flavoenzymes* (Müller, F., Ed.) pp 543−556, CRC Press, Boca Raton, FL.
18. Gassner, G. T., Ballou, D. P., Landrum, G. A., and Whittaker, J. W. (1993) *Biochemistry 32*, 4820−4825.
19. Rieske, J. S., McLennan, D. H., and Coleman, R. (1964) *Biochem. Biophys. Res. Commun. 15*, 338−344.
20. Fee, J. A., Kuila, D., Mather, M. W., and Yoshida, T. (1986) *Biochim. Biophys. Acta 853*, 153−185.
21. Cline, J. F., Hoffman, B. M., Mims, W. B., LaHaie, E., Ballou, D. P., and Fee, J. A. (1985) *J. Biol. Chem. 260*, 3251−3254.
22. Gurbiel, R. J., Batie, C. J., Sivaraja, M., True, A. E., Fee, J. A., Hoffman, B. M., and Ballou, D. P. (1989) *Biochemistry 28*, 4861−4871.
23. Gurbiel, R. J., Doan, P. E., Gassner, G. T., Macke, T. J., Case, D. A., Ohnishi, T., Fee, J. A., Ballou, D. P., and Hoffman, B. M. (1996) *Biochemistry 35*, 7834−7845.
24. Britt, R. D., Sauer, K., Klein, M. P., Knaff, D. B., Kriauciunas, A., Yu, C. A., Yu, L., and Malkin, R. (1991) *Biochemistry 30*, 1892−1901.
25. Kuila, D., Fee, J. A., Schoonover, J. R., Woodruff, W. H., Batie, C. J., and Ballou, D. P. (1987) *J. Am. Chem. Soc. 109*, 1559.
26. Tsang, H. T., Batie, C. J., Ballou, D. P., and Penner-Hahn, J. E. (1989) *Biochemistry 28*, 7233−7240.
27. Kauppi, B., Lee, K., Carredano, E., Parales, R. E., Gibson, D. T., Eklund, H., and Ramaswamy, S. (1998) *Structure 6*, 571−586.
28. Iwata, S., Saynovits, M., Link, T. A., and Michel, H. (1996) *Structure 4*, 576−579.
29. Carrell, C. J., Zhang, H., Cramer, W. A., and Smith, J. L. (1997) *Structure 5*, 1613−1625.
30. Batie, C. J., and Ballou, D. P. (1990) *Methods Enzymol. 188*, 61−70.
31. Tsang, H. T., Batie, C. J., Ballou, D. P., and Penner-Hahn, J. E. (1996) *J. Biol. Inorg. Chem. 1*, 24−33.
32. Pavel, E. G., Martins, L. J., Ellis, W. R., and Solomon, E. I. (1994) *Chem. Biol. 1*, 173−183.
33. Bertini, I., Luchinat, C., Mincione, G., Parigi, G., Gassner, G. T., and Ballou, D. P. (1996) *J. Biol. Inorg. Chem. 1*, 468−475.
34. Sono, M., Roach, M. P., Coulter, E. D., and Dawson, J. H. (1996) *Chem. Rev. 96*, 2841−2887.
35. Bull, C., and Ballou, D. P. (1981) *J. Biol. Chem. 256*, 12673−12680.
36. Hagen, W. R., Hearshen, R. H., Sands, R. H., and Dunham, W. R. (1985) *J. Magn. Reson. 61*, 220−232.
37. Hagen, W. R., Hearshen, D. O., Harding, L. J., and Dunham, W. R. (1985) *J. Magn. Reson. 61*, 233−244.
38. Schepler, K. L., Dunham, W. R., Sands, R. H., Fee, J. A., and Abeles, R. H. (1975) *Biochim. Biophys. Acta 397*, 510−518.
39. Ruzicka, F. J., Beinert, H., Schepler, K. L., Dunham, W. R., and Sands, R. H. (1975) *Proc. Natl. Acad. Sci. U.S.A. 72*, 2886−2890.
40. Sands, R. H., and Dunham, W. R. (1975) *Q. Rev. Biophys. 7*, 443−504.
41. Gibson, J. F., Hall, D. O., Thornley, J. H. M., and Whatley, F. R. (1966) *Proc. Natl. Acad. Sci. U.S.A. 56*, 987−990.
42. Stevenson, R. C. (1984) *J. Magn. Reson. 57*, 24−42.
43. Gassner, G. T. (1995) Ph.D. Thesis, University of Michigan.
44. Solomon, E. I., Sundaram, U. M., and Machonikin, T. E. (1996) *Chem. Rev. 96*, 2563−2606.
45. Ming, L. J., Que, L., Kriauciunas, A., Frolik, C. A., and Chen, V. J. (1990) *Inorg. Chem.* 1111−1112.
46. Lever, A. B. P. (1986) *Inorganic Electronic Spectroscopy*, 2nd ed., Elsevier, New York.
47. Veldink, G. A., and Vliegenthart, J. F. G. (1984) *Adv. Inorg. Biochem. 6*, 139−161.
48. Slykhouse, T. O., and Fee, J. A. (1976) *J. Biol. Chem. 251*, 5472−5477.
49. Zhang, Y., Gebhard, M. S., and Solomon, E. I. (1991) *J. Am. Chem. Soc. 113*, 5162−5175.
50. Erlandsen, H., Fusetti, F., Martinez, A., Hough, E., Flatmark, T., and Stevens, R. C. (1997) *Nat. Struct. Biol. 4*, 995−1000.
51. Goodwill, K. E., Sabatier, C., Marks, C., Raag, R., Fitzpatrick, P. F., and Stevens, R. C. (1997) *Nat. Struct. Biol. 4*, 578−585.
52. Morota, J. J. A., and Shiman, R. (1984) *Biochemistry 23*, 1303−1311.
53. Ohlendorf, D. H., Lipscomb, J. D., and Weber, P. C. (1988) *Nature 336*, 403−405.
54. Ohlendorf, D. H., Orville, A. M., and Lipscomb, J. D. (1994) *J. Mol. Biol. 244*, 586−608.
55. Bertrand, P., Guigliarelli, B., Gayda, J. P., Beardwood, P., and Gibson, J. F. (1985) *Biochim. Biophys. Acta 831*, 261−266.
56. Chang, H.-K., and Zylstra, G. J. (1998) *J. Bacteriol. 180*, 6529−6537.
57. Bernhardt, F. H., Ruf, H. H., and Staudinger, H. (1971) *Hoppe-Seyler's Z. Physiol. Chem. 352*, 1091−1099.
58. Twilfer, H., Bernhardt, F. H., and Gersonde, K. (1981) *Eur. J. Biochem. 119*, 595−602.
59. Taylor, J. S., and Coleman, J. E. (1971) *J. Biol. Chem. 246*, 7058−7067.
60. Taylor, J. S., and Coleman, J. E. (1973) *J. Biol. Chem. 248*, 749−755.
61. Taylor, J. S., and Coleman, J. E. (1972) *Proc. Natl. Acad. Sci. U.S.A. 69*, 859−862.
62. Rotilio, G., Morpurgo, L., Giovagnoli, C., Calabrese, L., and Mondovi, B. (1972) *Biochemistry 11*, 2187−2192.
63. Balasubramanian, S., Carr, R. T., Bender, C. J., Peisach, J., and Benkovic, S. J. (1994) *Biochemistry 33*, 8532−8537.
64. Jiang, F., Peisach, J., Ming, L. J., Que, L., Jr., and Chen, V. J. (1991) *Biochemistry 30*, 11437−11445.
65. Neidle, E. L., Hartnett, C., Ornston, L. N., Bairoch, A., Rekik, M., and Harayama, S. (1991) *J. Bacteriol. 173*, 5385−5395.
66. Jiang, H., Parales, R. E., Lynch, N. A., and Gibson, D. T. (1996) *J. Bacteriol. 178*, 3133−3139.
67. Nomura, Y., Nakagawa, M., Ogawa, N., Harashima, S., and Oshima, Y. (1992) *J. Ferment. Bioeng. 74*, 333−344.
68. Mason, J. R., Butler, C. S., Cammack, R., and Shergill, J. K. (1997) *Biochem. Soc. Trans. 25*, 90−95.
69. Boyington, J. C., Gaffney, B. J., and Amzel, L. M. (1993) *Science 260*, 1482−1486.
70. Minor, W., Steczko, J., Bolin, J. T., Otwinowski, Z., and Axelrod, B. (1993) *Biochemistry 32*, 6320−6323.
71. Han, S., Eltis, L. D., Timmis, K. N., Muchmore, S. W., and Bolin, J. T. (1995) *Science 270*, 976−980.
72. Senda, T., Sugiyama, K., Narita, H., Yamamoto, T., Kimbara, K., Fukuda, M., Sato, M., Yano, K., and Mitsui, Y. (1996) *J. Mol. Biol. 255*, 735−752.
73. Roach, P. L., Clifton, I. J., Fulop, V., Harlos, K., Barton, G. J., Hajdu, J., Andersson, I., Schofield, C. J., and Baldwin, J. E. (1995) *Nature 375*, 700−704.

74. Valegard, K., Terwisscha van Scheltinga, A. C., Lloyds, M. D., Hara, T., Ramaswamy, S., Perrakis, A., Thompson, A., Lee, H.-J., Baldwin, J. E., Schofield, C. J., Hajdu, J., and Andersson, I. (1998) *Nature 394*, 805−809.
75. Roach, P. L., Clifton, I. J., Hensgens, C. M., Shibata, N., Schofield, C. J., Hajdu, J., and Baldwin, J. E. (1997) *Nature 387*, 827−830.
76. Hegg, E. L., and Que, L., Jr. (1997) *Eur. J. Biochem. 250*, 625−629.
77. Slappendel, S., Veldink, G. A., Vliegenthart, J. F. G., Aasa, R., and Malmstrom, B. G. (1981) *Biochim. Biophys. Acta 667*, 77−86.
78. Tierney, D. L., Gassner, G. T., Luchinat, C., Bertini, I., Ballou, D. P., and Penner-Hahn, J. E. (1999) *Biochemistry 38*, 11051−11061.

BI9904499